Available online at www.sciencedirect.com
SCIENCE DIRECT
International Journal of Multiphase Flow 32 (2006) 593–605
International Journal of Multiphase Flow
www.elsevier.com/locate/ijmulflow

Effect of a liquid dispersed phase on the wall flow structure in static mixer

J. Legrand *, K. Hirech, A. Arhaliass

Université de Nantes, CNRS, GEPEA, UMR6144, CRTT – BP 406, 44602 Saint-Nazaire Cedex, France

Received 10 October 2004; received in revised form 12 February 2006

Abstract

The effect of a liquid dispersed on the wall flow structure in static mixer is analyzed by using an electrochemical method. Both laminar and turbulent flows have been investigated. The axial wall velocity gradient and turbulent intensity have been studied along the static mixer in both flow regimes and for different dispersed phase concentrations. The spectral analysis of the wall velocity gradient fluctuations was analyzed in the turbulent regime. For volume fraction higher than 5%, the effect of the dispersed liquid phase is very important for all the studied parameters. The turbulence associated to the dispersed phase leads to an increase of the energy dissipation in the static mixer and also to a modification of energy dissipation mechanism.

Keywords: Electrochemical method; Liquid–liquid dispersion; Spectral analysis; Static mixer; Turbulence; Wall shear rate

1. Introduction

The effect of a fluid or solid dispersed phase on flow turbulence is due to different parameters: particle sizes, physicochemical properties of both phases, shift velocity, droplet deformation, breakage and coalescence phenomena,... Yuan and Michaelides (1992) have summarized six mechanisms which contribute to modify turbulence characteristics in two-phase systems:

- turbulent kinetic energy dissipation by the particles,
- apparent viscosity increase due to the dispersed phase,
- particle wake,
- fluid mass-added to particles,
- velocity gradients between particles,
- deformation of dispersed phase.

* Corresponding author. Tel.: +33 240 17 26 33; fax: +33 240 17 26 18.
E-mail address: jack.legrand@gepea.univ-nantes.fr (J. Legrand).

0301-9322/$ - see front matter © 2006 Elsevier Ltd. All rights reserved.
doi:10.1016/j.ijmultiphaseflow.2006.02.002

Several studies have been undertaken to analyze how turbulence and gas bubbles influence each other. Serizawa et al. (1975) experimentally studied the influence of bubbles on turbulence and the effect of the latter on the velocity and void fraction. Theofanous and Sullivan (1982) examined the enhancement of liquid turbulence by flowing bubbles. Nikotopoulos and Michaelides (1995) showed that the eddy diffusivity was enhanced due to variation of the density by considering the gas–liquid mixture as a homogeneous fluid of variable density across the pipe cross-section. Nakoryakov et al. (1981) and Souhar (1989) made measurements of wall shear stress in bubbly pipe flow. Souhar (1989) studied the effect of bubbles on energy spectra. Significant modification of turbulence were observed in the different studies (Gore and Crowe, 1989; Hestroni, 1989; Lance and Bataille, 1991; Mizukami et al., 1992; Parthasarathy and Faeth, 1987; Souhar, 1989; Theofanous and Sullivan, 1982; Yarin and Hestroni, 1994; Yuan and Michaelides, 1992; Hosokawa and Tomiyama, 2004).

Few studies are devoted to the effect of the dispersed phase on liquid–liquid flows. Nadler and Mewes (1997) reported that the pressure drop in pipeline flow of two immiscible liquids strongly depends on the flow regime. Yuge and Hagiwara (2004) visualized by direct numerical simulation the secondary flow in the droplet wake. Moreover, liquid–liquid dispersions with high volume fractions of the dispersed phase often behave as non-Newtonian shear thinning fluids (Loewenberg, 1998). Tsouri and Tavlarides (1994) observed a damping effect of the dispersed phase concentration on the turbulent fluctuations. The damping rate is proportional to $(1-\alpha)^{-1}$.

Static mixers are applied in wide range of industrial processes, but the fundamental understanding of flow and mixing in static mixers, is however poor (Godfrey, 1992). The scarcity of information about static mixer flow is due to their complex structure, which makes non-intrusive investigation difficult. One of the most important applications of the static mixers is for immiscible liquid–liquid dispersion. Many research works were done in order to predict the drop size distribution obtained with different types of static mixer (Berkman and Calabrese, 1988; Haas, 1987; Legrand et al., 2001; Maa and Hsu, 1996; Middleman, 1974). However, to the best of our knowledge, no work has been devoted to the analysis of the effect of a dispersed phase on the flow in static mixers. In the present work, we have investigated the flow through static mixers by using non-intrusive electrochemical method, which allows to obtain wall shear stress along the housing tube of the static mixer elements. In a previous work (Hirech et al., 2003), we analysed the one-phase flow through SMX Sulzer static mixer with the same experimental method. In particular, we characterized the flow regimes: laminar regime for $Re_{\text{pore}} < 200$ and turbulent regime for $Re_{\text{pore}} > 1500$–3000. The pore Reynolds number, Re_{pore}, which takes into account the geometric structure of the static mixer, was defined by Morançais et al. (1999) by considering the static mixer as a porous medium and by using a capillary model. The objective of this work is to analyse the effect of a dispersed phase on the different flow characteristics in both laminar and turbulent flow regimes.

2. Materials and methods

2.1. Hydraulic loop and test cell

The experimental set-up is shown in Fig. 1. The two-phase mixture was prepared in a stirred tank with a temperature control system. The two-phase mixture was pumped through flowmeters to the test cell, which consisted of a calming section and a measured section containing the static mixer elements. The two-phase mixture was then returned to the stirred tank. The two-phase mixture flowrate was varied between 0.04 and 6 m^3/h. The test section contained four SMX Sulzer static mixer elements (Fig. 2) of 51.6 mm of nominal diameter, corresponding to the housing tube diameter. A SMX static mixer element consisted of corrugated plates perpendicular to each other and assembled at 90° from the flow axis (Fig. 2). The series of blades divide the passing fluid into layers and spread them over the pipe cross-section. The geometrical characteristics (pore diameter, d_p, and tortuosity factor, T, corresponding to the ratio of the mean length covered by the fluid to the mixer length) of the SMX static mixer have been determined through pressure drop measurements by using a capillary model (Morançais et al., 1999). The porosity, ε, of the static mixer is equal to 0.90, the pore diameter, d_p, to 15.15 mm and the tortuosity factor, T, to 1.46. The flow characteristics were characterized by using a pore Reynolds number, defined from a capillary model (Morançais et al., 1999) as:

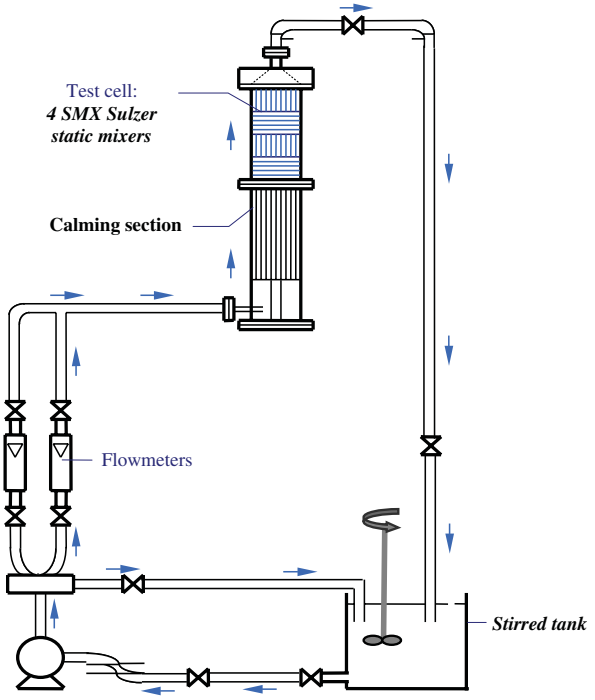

Fig. 1. Experimental set-up.

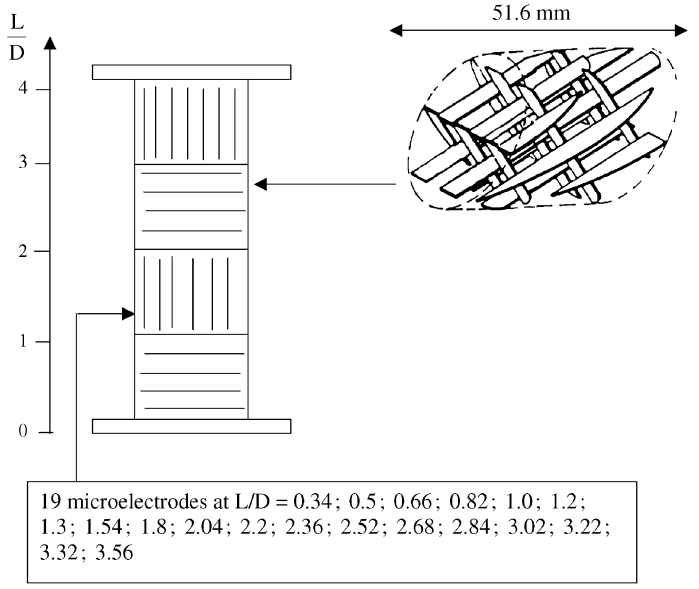

Fig. 2. Description of the SMX Sulzer static mixer.

$$Re_{\text{pore}} = \frac{\rho u_0 T d_p}{\varepsilon \eta} \tag{1}$$

where ρ and η are respectively the density and the dynamic viscosity of the continuous phase and u_0 is the superficial velocity of the continuous phase.

2.2. The electrochemical method

The electrochemical method is a non-intrusive experimental technique, which allows to study wall flow dynamics and to determine the local near-wall flow characteristics such as the wall shear stress or the wall-turbulence characteristics (Hanratty and Campbell, 1983). The electrochemical method was carried out by using microelectrodes in order to locally investigate the flow dynamics. Nineteen microelectrodes were mounted flush to the surface of the housing tube of the static mixers (Fig. 2). The electrochemical method is based on a simple transfer model of an active ion from the bulk of the electrolyte (the continuous phase) to the microelectrode. Under definite conditions (Hanratty and Campbell, 1983), the current delivered by the microelectrodes is controlled by diffusion only. The mean value of the wall velocity gradient, $\overline{S}$, is related (Hanratty and Campbell, 1983) to the mean value of the diffusional current, $\overline{I}$:

$$\overline{S} = \left[\frac{\overline{I}}{0.677nFC_0D_{\mathrm{iff}}^{2/3}d^{5/3}}\right] \tag{2}$$

where C_0 is the concentration of the active ion, n the number of electrons involved in the electrochemical reaction, F the Faraday number, d the diameter of the microelectrode and D_{iff} the diffusion coefficient. The wall-turbulence characteristics can be obtained from the fluctuations of the diffusional current. The power spectral density of the diffusional current fluctuations is related to that of the wall velocity gradient fluctuations through a transfer function (Deslouis et al., 1990). The transfer function was established by assuming that the diffusional boundary layer acts as high-frequency pass filter for the wall velocity gradient fluctuations (Deslouis et al., 1990). The acquisition system consisted of a current-potential converter, which also allowed the microelectrodes polarization and a digital audiotape TEKELEC RD-145 T permitting the simultaneous recording of sixteen signals. A spectral analysis was applied to the fluctuating diffusional current obtained from the microelectrodes.

2.3. Working fluids

Two continuous phases were used in order to obtain different viscosity solutions for a wider domain of the pore Reynolds number. The two electrolytes consisted of an aqueous solution of potassium ferro and ferricyanide and potassium nitrate. The increase of the viscosity was obtained by adding glycerol in the electrolyte. The characteristics of the two electrolytes are given in Table 1. The electrochemical reaction carried out on the microelectrodes was the cathodic reduction of the potassium ferricyanide. The dispersed phase was an oil solution (Table 1). The interfacial tension between the two immiscible phases was equal to 16.4 mN/m at 30 °C. Different volume fractions of the dispersed phase were prepared: 0.1%; 1.0%; 5.0%; 10%; 15% and 30%. The liquid–liquid dispersions behave as Newtonian fluids for all the volume fractions of the dispersed phase.

2.4. Determination of size distribution of the dispersed phase

The on-line measurement of size distribution of liquid droplets in concentrated liquid–liquid dispersions is very difficult. The stabilisation of the liquid–liquid dispersion using microencapsulation by interfacial polymerisation (Legrand et al., 2001) or by acetylation (Zhao et al., 1993) can be a solution. To avoid side-

Table 1
Physical properties of the working fluids

Fluids	Potassium ferri and ferrocyanide (M)	Sodium nitrate (M)	Temperature (°C)	Density (ρ) (kg/m^3)	Viscosity (η) (mPa s)	Diffusion coefficient (Diff) (m^2/s)
Continuous phase 1: aqueous solution	5×10^{-3}	1	30	1053	0.86	7.45×10^{-10}
Continuous phase: aqueous solution of glycerol (62%)	5×10^{-2}	1	30	1210	8.3	5.61×10^{-11}
Oil dispersed phase	/	/	30	801	3.2	/

reactions with the electrolyte, we carried out a microencapsulation technique by acetylation (Zhao et al., 1993). The principle is based on a fast reaction between a mixture of two aldehydes (isobutyraldehyde and butyraldehyde) contained in oil phase and a polyvinylalcohol in the aqueous phase. The acelytation reaction leads to a polymeric film around the oil droplets, which allows to observe the microcapsules. The dispersed phase consisting of a mixture of 1.96% of isobutyraldehyde and 1.96% o butyraldehyde in oil was mixed in the electrolyte in the hydraulic loop containing the static mixer (Fig. 1). After the stabilisation of the liquid–liquid dispersion, a sample of the dispersion was taken in a flask containing a 2% polyvinyl alcohol aqueous solution at acidic pH. The analysis of the microcapsules drop size were made by laser granulometer and by image analysis using the experimental technique described by Legrand et al. (1995). An example of the size distribution obtained during the experiments is given in Fig. 3.

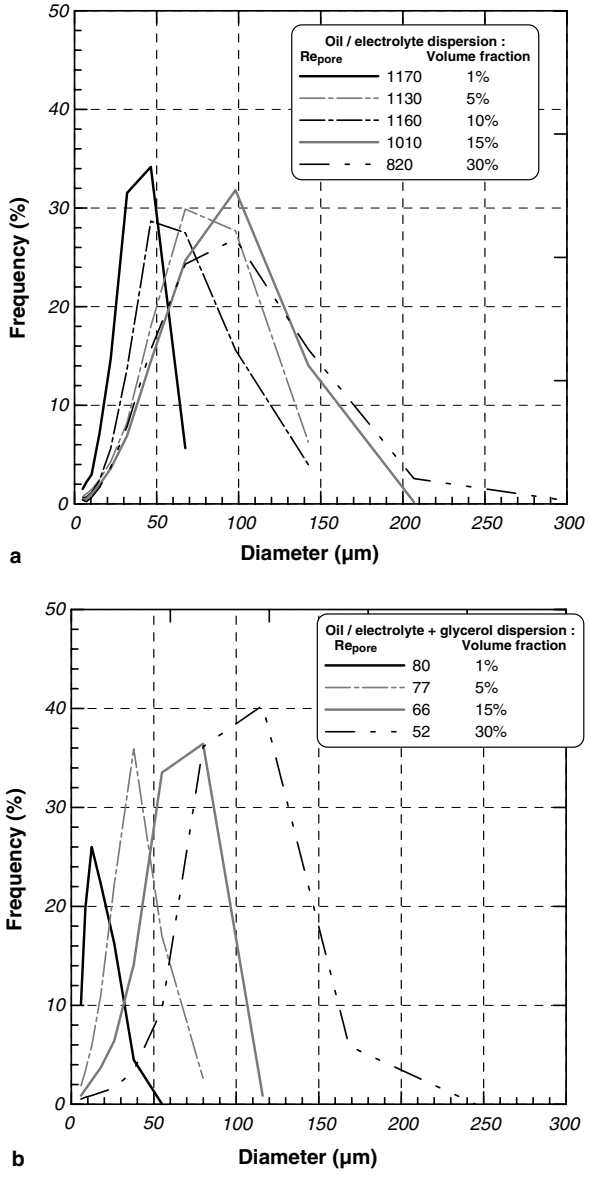

Fig. 3. Granulometric distribution of the dispersed phase (a) in turbulent and (b) in laminar flow regime.

3. Results and discussion

3.1. Effect of a dispersed phase on wall velocity gradient fluctuations

The two-phase systems used were a dispersion of oil in glycerol aqueous electrolytic solution for laminar flow and in electrolyte for turbulent flow with different volume oil fractions. The laminar flow regime in SMX Sulzer static mixer was defined in one-phase flow (Hirech et al., 2003) for pore Reynolds number less than 200. The laminar flow regime is characterized by time-constant evolution of the diffusional limiting current recorded at the different microelectrodes. The time-evolution of the diffusional current is given in Figs. 4 and 5 for low and high pore Reynolds numbers and for an axial location of the microelectrode corresponding to a developed flow in the static mixer (Hirech et al., 2003). For laminar flow regime ($Re_{pore} < 200$), the diffusional current is time-independent for volume fraction of the dispersed phase less than 5%. The dispersed phase has no effect on the fluctuation rate of the diffusional current, which is similar to the one obtained in one-phase flow (Fig. 4). For volume fractions greater than 5%, time-fluctuations appear on the diffusional current recordings. Fluctuations rates increase with the volumic fraction (Fig. 4). The effect of the dispersed phase on the fluctuation rate of the diffusional current is very low for turbulent flow regime (Fig. 5). The fluctuation rate of the velocity gradient, corresponding to the rms of the wall velocity gradient, is shown in Fig. 6 for both flow regimes. The effect of the dispersed phase is more important for low pore Reynolds number values. The liquid droplets act as turbulence promoters. In laminar flow regime ($Re_p < 200$), the pseudo-turbulence is only due to the dispersed phase. The increase of the pseudo-turbulence is more important for low values of the volume fraction ($\alpha = 0$–10%). No significant effect is shown for an increase of volume fraction between 10% and 30% (Fig. 6a). In the transition flow regime, the dispersed phase has a significant effect on the fluctuation rate (Fig. 6a and b), which decreases with an increase of the pore Reynolds number. Two phenomena are associated to the increase of the pore Reynolds number: a decrease of droplets size distribution and an increase of the turbulence intensity due to the static mixer. However, the effect of the size distribution of liquid droplets is difficult to investigate, because of the dependence of the size distribution with both pore Reynolds number and volume fraction (Fig. 3). As shown in Fig. 6, the effect of the volume fraction on the fluctuation rate is not really defined. For turbulent flow regime ($Re_{pore} > 1500$–3000), the dispersed phase has no effect on the fluctuation rate, which is essentially due to turbulence production in the static mixer (Fig. 6b).

3.2. Effect of the dispersed phase on mean wall velocity gradients

The evolution of the mean wall velocity gradient along the static mixers is shown in Fig. 7. The evolution is the same for the different pore Reynolds numbers and for the different volume fractions of the dispersed phase and similar to the one for one-phase flow. The periodic evolution of the wall velocity gradient is generated by the static mixer geometry (Fig. 2), which imposes the flow direction and the contraction–expansion flow phenomena. However, the amplitude of the wall velocity gradient is dependent on the presence of the dispersed phase (Fig. 8). For low dispersed phase concentration (<5%), the wall velocity gradient is independent of the dispersed phase. For higher concentrations, the wall velocity gradient monotonically increases with the volume fraction. The mixing of the continuous phase is enhanced by the oil droplets. Few studies have delt with the effect of a dispersed phase on wall transport phenomena. Nakoryakov et al. (1981) obtained for a gas–liquid tubular flow the following expression:

$$\frac{S_{di}}{S_{mono}} = (1 - 0.83\alpha)^{-1.53} \tag{3}$$

where S_{di} and S_{mono} are respectively the wall shear rate in two-phase and one-phase flow. Eq. (3) also shows a monotonous increase of shear rate with α. Nakoryakov et al. (1981) also observed a deformation of the velocity profile in two-phase flow and an increase of the liquid velocity due to the presence of the dispersed phase and consequently to an increase of the wall velocity gradient.

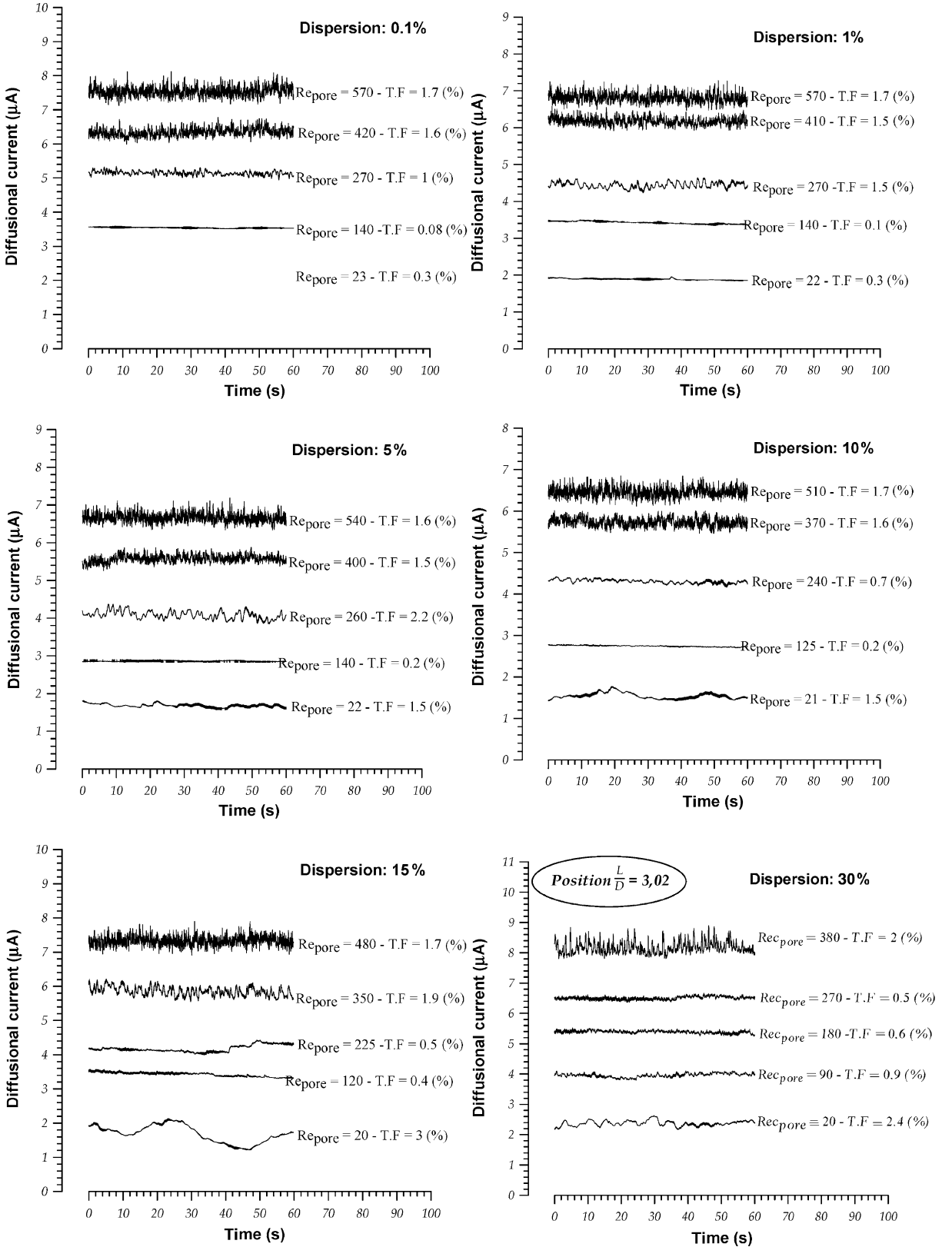

Fig. 4. Time-variation of the limiting diffusional current for different dispersed flows concentrations and for low Reynolds numbers.

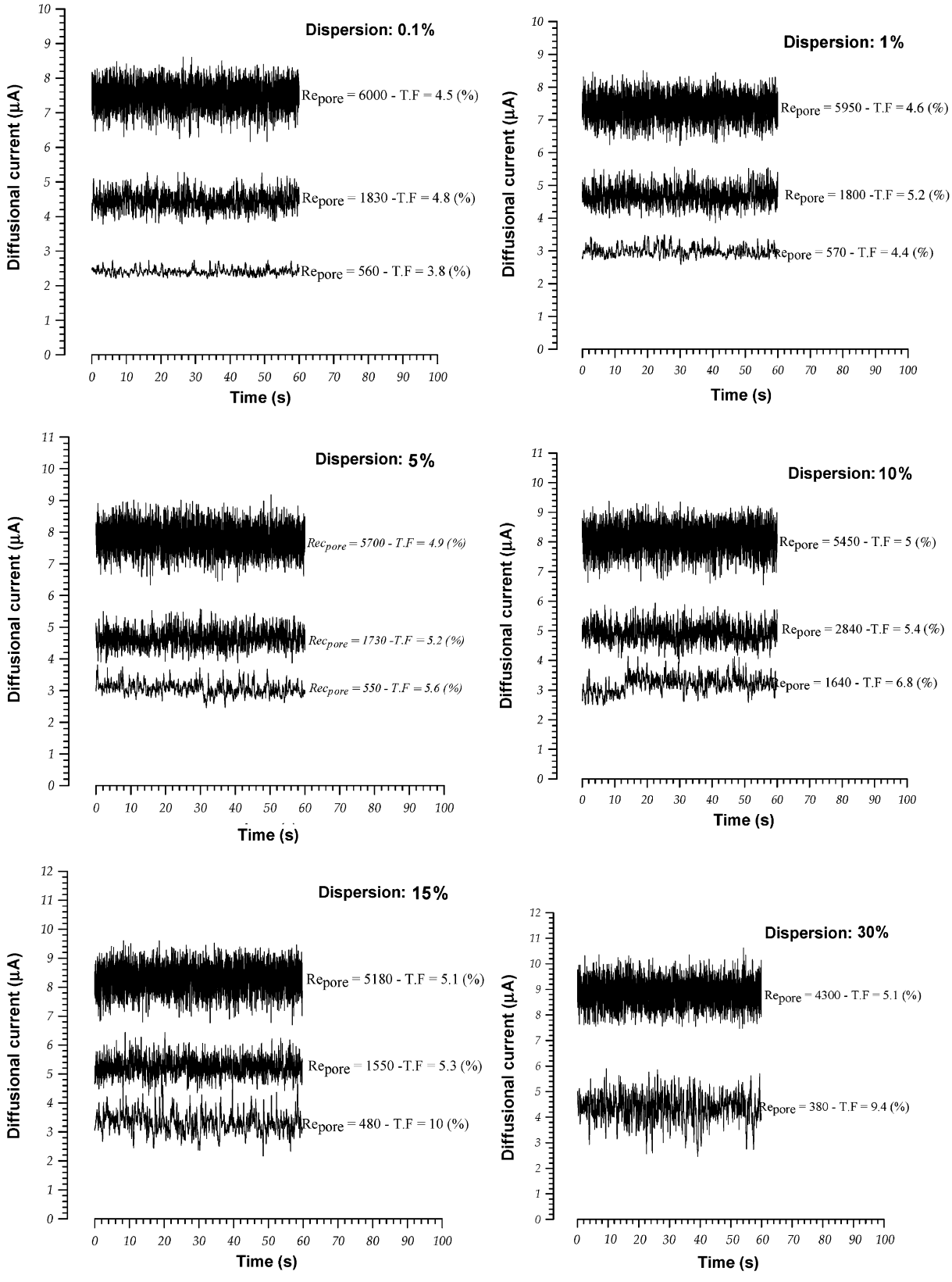

Fig. 5. Time-evolution of the limiting diffusional current for different dispersed phase concentrations and for high Reynolds numbers.

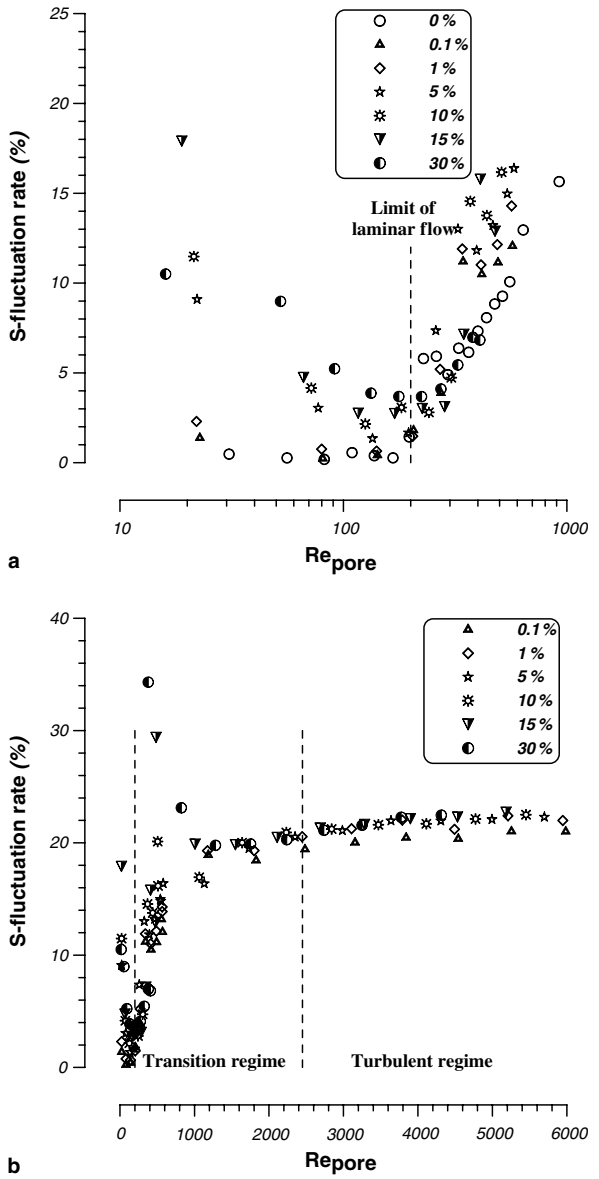

Fig. 6. Evolution of the fluctuation rate of wall velocity gradient with Reynolds number (a) for low Reynolds numbers; (b) for high Reynolds number.

3.3. Spectral analysis of the wall velocity gradient fluctuations

The variation of the power spectra as a function of the Reynolds number is given in Fig. 9 for different volume fractions. The power spectra evolution is rather similar for the different experimental conditions. The low frequencies domain is defined by a plateau without characteristic frequency and no specific evolution can be observed for the different volume fractions of the dispersed phase. For the high frequencies domain, the energy cascade for $\alpha < 5\%$ is similar to the one obtained in one-phase flow. However the dissipation domain is modified for higher volume fractions (Fig. 9b and c). The energetic level and the frequency domain width increase with α. The deformation of the power spectrum could be attributed to the formation of eddies in the droplets wake (Yuge and Hagiwara, 2004), to the dissipation of the turbulent kinetic energy by the droplets which have a size of the same order of magnitude as the Kolmogorov scale and to the increase of the

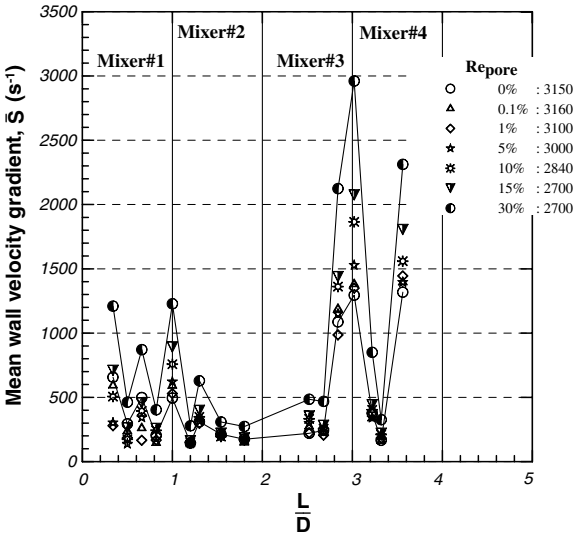

Fig. 7. Axial variation of the mean wall velocity gradient in the static mixer.

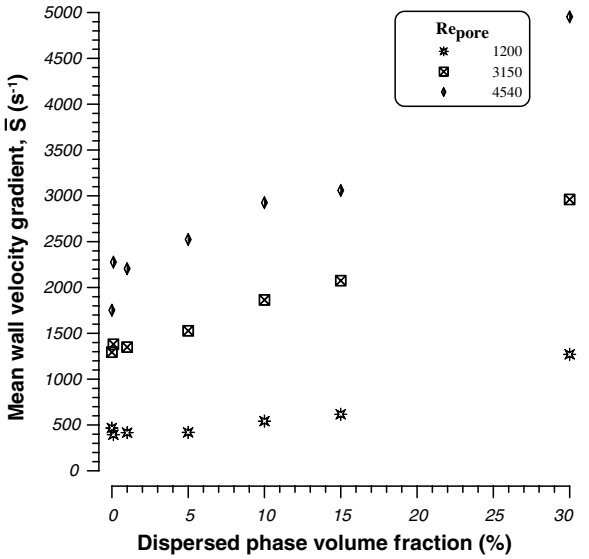

Fig. 8. Variation of the wall velocity gradient with the volume fraction of the dispersed phase for $L/D = 3.02$.

viscous dissipation due to the increase in the apparent viscosity of the oil–water dispersion. Similar observations were made by Souhar (1989) for turbulent gas–liquid flow. According to the energy cascade, the energy is transported from the large structures to the smallest ones up to the viscous dissipation. When the droplets are smaller than turbulent structures, they are simply convected. When the size of the droplets is greater than the eddies size, they interact with the turbulent structures, which results in the increase of the kinetic energy transfer in the high-frequency domain and to the break-up of the droplets. Jairazbhoy and Tavlarides (1995) have studied the mutual interactions between a drop population and a homogeneous turbulent energy spectrum by using a two-phase cascade numerical model. They have also found that the phase fraction is the most significant parameter. The crossing-trajectories, corresponding to the drop migration from one given correlated fluid region to another, could explain the particle-fluid interactions, which contribute to modify the spectrum, especially at high wave numbers.

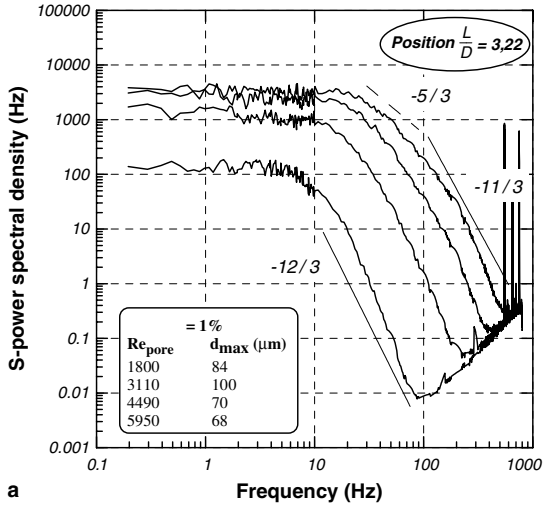

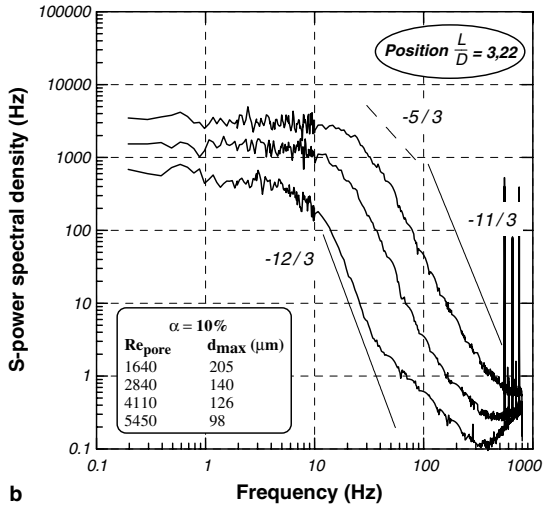

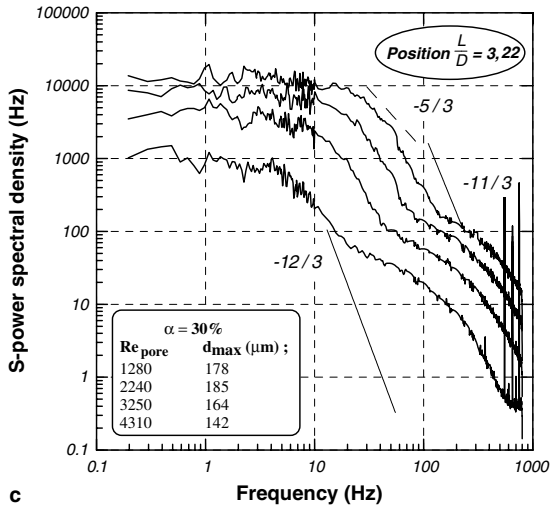

Fig. 9. Power spectral density of the wall velocity gradient (a) for $\alpha = 1\%$; (b) for $\alpha = 10\%$; (c) for $\alpha = 30\%$.

For the highest volume fraction (Fig. 9c), the evolution of the power spectra with the frequency is very different from the one obtained in one-phase flow. The evolution is non monotonous in the dissipation domain: the power-law varies with f^{-1} for the larger eddies, followed by $f^{-11/3}$ variation for the smaller eddies. This evolution is due to the interactions between droplets and turbulent eddies associated to the break-up phenomena occurring in static mixer. The influence of a dispersed phase on the power spectra was already observed in gas–liquid flow by Souhar (1989) and Lance and Bataille (1991) who also obtained a similar f^{-1} and then $f^{-7/3}$ (or $f^{-8/3}$) evolution instead of the classical $f^{-5/3}$ law.

The kinetic energy dissipation rate, ε_D, can be obtained from power spectral density. The evolution of the dissipation rate along the static mixer is shown in Fig. 10 for a given Reynolds number and for different volume fractions. The axial evolution of the dissipation rate is not dependent on the volume fraction of the dispersed phase but only on the geometry of the static mixer. High dissipation rates are obtained in the open regions of the static mixer with recirculation flows and low dissipation rates are observed in the region where the blades mixer are near the wall. The dissipation rate increases with the volume fraction for all the axial locations and the mean axial dissipation rate is equal to 0.10; 0.18; 0.26; 0.55; 3.98 and 25.10 m^2/s^3 for respectively $\alpha = 0\%$; 1%; 5%; 10%; 15% and 30%. The increase of the energy dissipation rate is associated with a decrease of the Kolmogorov microscale, m_K:

$$m_K = \left(\frac{\upsilon^3}{\varepsilon_D}\right) \tag{4}$$

m_K varies from 48 μm to 16 μm when α increases from 0% to 30%. According to Fig. 3, the droplet size has the same order of magnitude as the Kolmogorov microscale for low dispersed phase concentration, and is greater for high concentration. In this case, the droplets–turbulent eddies interactions significantly modify the energy cascade (Fig. 9). This evolution of the Kolmogorov microscale was also observed by Souhar (1989) and Lance and Bataille (1991).

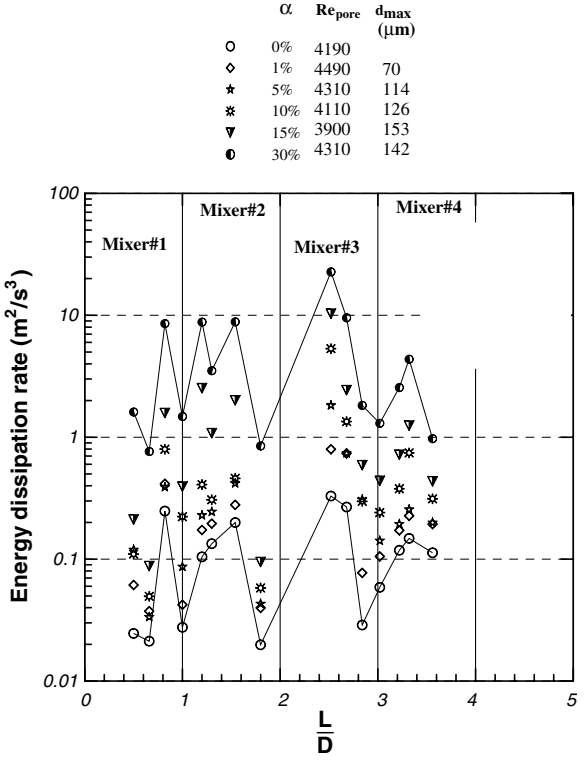

Fig. 10. Axial variation of the local energy dissipation rate.

4. Conclusion

The effect of the dispersed phase on the flow structure was studied with respect to the flow regime obtained in one-phase flow. For low dispersed phase concentration (<1%), the laminar flow regime keeps its character. For higher concentrations, the turbulent intensity is increased for both flow regimes. The wall velocity gradient exhibits a similar axial evolution along the static mixer in one-phase and two-phase flows, with a monotonous increase of the amplitude with the volume fraction. The same results are obtained for the local energy dissipation rate. The spectral characteristics are deeply modified for high volume fractions. The frequency domain is enlarged and the energy dissipation scheme characterized by f^{-1} and $f^{-11/3}$ evolution of the power spectral density.

References

Berkman, P.D., Calabrese, R.V., 1988. Dispersion of viscous liquids by turbulent flow in static mixer. AIChE J. 34, 602–609.

Deslouis, C., Gil, O., Tribollet, B., 1990. Frequency response of electrochemical sensors to hydrodynamic fluctuation. J. Fluid Mech. 215, 85–100.

Godfrey, J.C., 1992. Static mixers. In: Harnby, N., Edwards, M.F., Nienow, A.W. (Eds.), Mixing in the Process Industries, second ed. Butterworth-Heinemann, Oxford, pp. 225–249.

Gore, R.A., Crowe, C.T., 1989. Effect of particle size on modulating turbulent intensity. Int. J. Multiphase Flow 15, 279–285.

Haas, P.A., 1987. Turbulent dispersion of aqueous drops in organic liquids. AIChE J. 33, 987–995.

Hanratty, T.J., Campbell, J.A., 1983. Measurement of wall shear stress. In: Goldstein, J. (Ed.), Fluid Mechanics Measurements. Hemisphere Publishing Corporation, Washington, pp. 559–615.

Hestroni, G., 1989. Particles–turbulence interaction. Int. J. Multiphase Flow 15, 735–746.

Hirech, K., Arhaliass, A., Legrand, J., 2003. An experimental investigation of flow regimes in SMX static mixer. Ind. Eng. Chem. Res. 42, 1478–1484.

Hosokawa, S., Tomiyama, A., 2004. Turbulence modification in gas–liquid and solid–liquid dispersed two-phase pipe flows. Int. J. Heat Fluid Flow 25, 489–498.

Jairazbhoy, V., Tavlarides, L.L., 1995. A cascade model for neutrally buoyant dispersed two-phase homogeneous turbulence – Numerical solution and results. Int J. Multiphase Flow 21, 485–500.

Lance, M., Bataille, J., 1991. Turbulence in liquid phase of a uniform bubbly air–water flow. J. Fluid Mech. 222, 95–118.

Legrand, J., Brujes, L., Carnelle, G., Phalip, P., 1995. Study of a microencapsulation process of a virucide agent by a solvent evaporation technique. J. Microencap. 12, 639–649.

Legrand, J., Morançais, P., Carnelle, G., 2001. Liquid–liquid dispersion in an SMX Sulzer static mixer. Chem. Eng. Res. Des. 79, 949–956.

Loewenberg, M., 1998. Numerical simulation of concentrated emulsion flows. J. Fluids Eng. 120, 824–832.

Maa, Y.F., Hsu, C., 1996. Liquid–liquid emulsification by static mixers for use in microencapsulation. J. Microencap. 13, 419–433.

Middleman, S., 1974. Drop size distributions produced by turbulent pipe flow of immiscible fluids through a static mixer. Ind. Eng. Chem. Proc. Des. Dev. 13, 78–83.

Mizukami, M., Parthasarathy, R.N., Faeth, G.M., 1992. Particle-generated turbulence in homogeneous dilute dispersed flows. Int. J. Multiphase Flow 18, 397–412.

Morançais, P., Hirech, K., Carnelle, G., Legrand, J., 1999. Friction factor in static mixer and determination of geometric parameters of SMX Sulzer mixers. Chem. Eng. Commun. 171, 77–93.

Nadler, M., Mewes, D., 1997. Flow induced emulsification in the flow of two immiscible liquids in horizontal pipes. Int. J. Multiphase Flow 23, 55–68.

Nakoryakov, J.E., Kashinsky, O.N., Burdukov, A.P., Odnoral, V.P., 1981. Local characteristics of upward gas–liquid flows. Int. J. Multiphase Flow 7, 63–81.

Nikotopoulos, D.E., Michaelides, E.E., 1995. Phenomenological model for dispersed bubbly flow in pipes. AIChE J. 41, 12–22.

Parthasarathy, R.N., Faeth, G., 1987. Structure of particle-laden turbulent water jets in still water. Int. J. Multiphase Flow 13, 699–716.

Serizawa, A., Kataoka, I., Michiyoshi, I., 1975. Turbulent structure of air–water bubbly flow. Int. J. Multiphase Flow 2, 221–259.

Souhar, M., 1989. Some turbulence quantities and energy spectra in the wall region in bubble flows. Phys. Fluids A 1, 1558–1565.

Theofanous, T.G., Sullivan, J., 1982. Turbulence in two-phase dispersed flows. J. Fluid Mech. 116, 343–362.

Tsouri, C., Tavlarides, L.L., 1994. Breakage and coalescence models for drops in turbulent dispersions. AIChE J. 40, 395–406.

Yarin, L., Hestroni, G., 1994. Turbulence intensity in dilute two-phase flows – I: effect of particle-size distribution on the turbulence of the carrier fluid. Int. J. Multiphase Flow 20, 1–15.

Yuan, Z., Michaelides, E.E., 1992. Turbulence modulation in particle flows – a theoretical approach. Int. J. Multiphase Flow 18, 779–785.

Yuge, T., Hagiwara, Y., 2004. The modifications of near-wall-turbulence structure and heat transfer by immiscible droplets in turbulent liquid–liquid two-phase flow. Int. J. Heat Fluid Flow 25, 471–480.

Zhao, W.Q., Pu, B.Y., Hartland, S., 1993. Measurement of drop size distribution in liquid–liquid dispersions by encapsulation. Chem. Eng. Sci. 48, 219–227.